Constraints on the Timing of Exhumation in the Colorado Front Range using Apatite and Zircon (U-Th)/He Thermochronometry

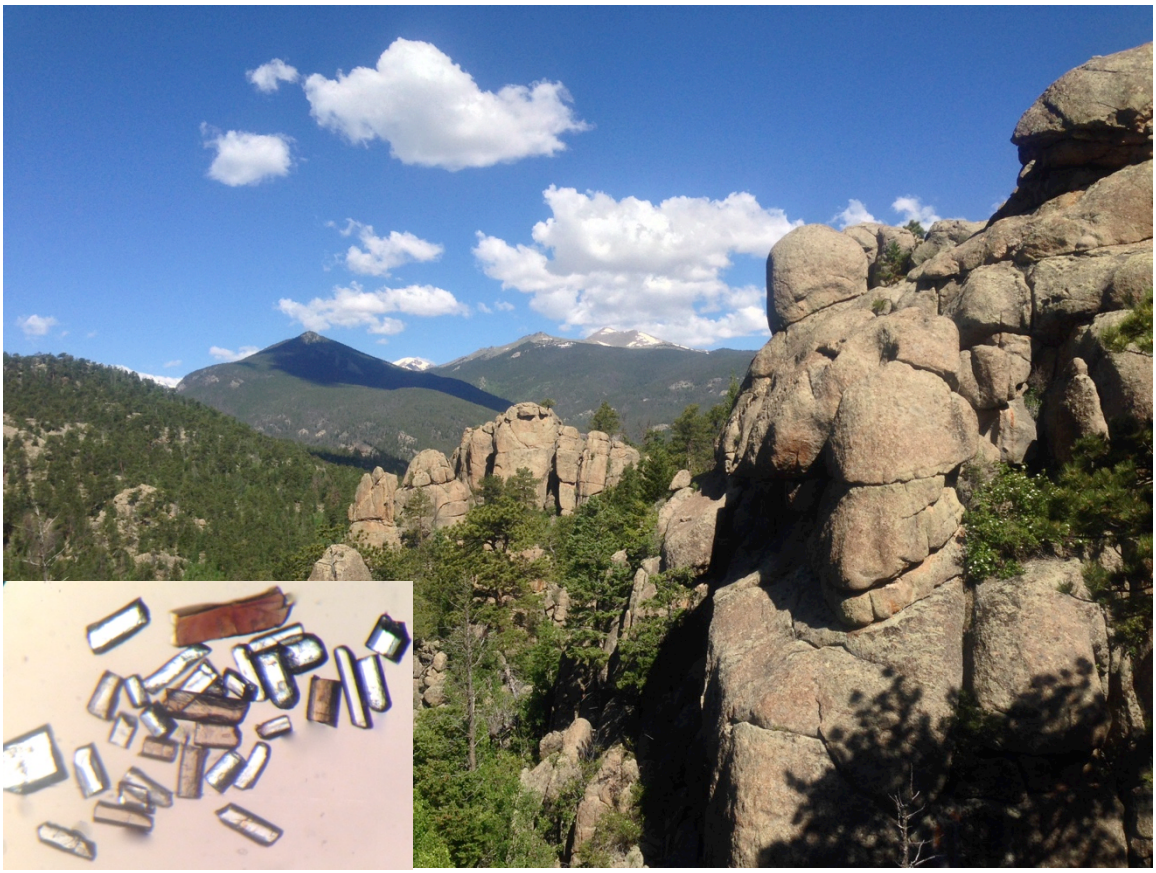

Thesis for Departmental Honors at the University of Colorado Boulder

David T. Liefert

Department of Geological Sciences

Defense Date: April 3rd, 2015

Defense Committee:

Thesis Advisor: Rebecca Flowers – Department of Geological Sciences
Committee Member: Charles Stern – Department of Geological Sciences
Committee Member: Suzanne Anderson – Department of Geography

Constraints on the Timing of Exhumation in the Colorado Front Range using Apatite and Zircon (U-Th)/He Thermochronometry

David T. Liefert

Department of Geological Sciences

ABSTRACT

Despite the prominence of the Rocky Mountains, questions remain about the timing and character of the most recent mountain building event in the Colorado Front Range, the Laramide Orogeny. This history can be investigated using (U-Th)/He thermochronology, a technique sensitive to low temperatures and the uppermost stages of cooling. I collected samples in three areas of the Front Range extending across an ~50 km long east-west transect, and acquired data for four samples from Big Thompson Canyon within the eastern portion of the sampled region. The apatite (U-Th)/He thermochronometer was applied because of its relatively low closure temperature (~70 °C) and potential for furthering our understanding of the effects of radiation damage on the dates acquired from zircon helium (ZHe) analyses. I additionally acquired zircon (U-Th)/He data when it became apparent that most apatite data were compromised by abundant mineral inclusions. 11 single grain apatite analyses for a single sample from Big Thompson Canyon yielded a mean apatite (U-Th)/He date of 66.5 ± 9.62 Ma. 15 single-grain zircon analyses for three samples from Big Thompson Canyon have mean dates ranging from 45.01 ± 7.24 Ma to 64.55 ± 11.13 Ma. The closure temperature of zircon is nominally ~180 ˚C, but may have been lowered in the studied grains as He retentivity decreased due to the accumulation of radiation damage. The similar dates of the zircon samples located at different elevations, as well as the overlap of zircon and apatite He dates, indicate rapid exhumation in the Colorado Front Range during the Late Cretaceous–Early Tertiary Laramide Orogeny.

Acknowledgements

First and foremost, I would like to thank Joshua Johnson for providing me the opportunity to create an honors thesis and guiding me through the writing process. I was hired by Joshua as a field and laboratory assistant and had the privilege of helping to acquire samples and data for his MSc thesis. I have gained invaluable experience working alongside Joshua as he has mentored me through research techniques and applying what I've learned to an honors thesis. I'd also like to thank Rebecca Flowers for providing me support and guidance from the inception of the project to the final revision. Both Joshua and Rebecca's patience and willingness to help have been instrumental in my efforts to complete this project and gain experience in research. I would like to additionally thank Jim Metcalf for his help in laboratory procedures, analytical analyses, and availability to answer questions throughout the research process. I would also like to thank Dr. Graham Baird and Dr. Shari Kelley for donating mineral separates to the study. And finally, I would like to thank Charles Stern for motivating and directing me through the process of an honors thesis, and Suzanne Anderson for her support and interest in my thesis topic.

CONTENTS

Chapter 1
Introduction

Introduction

Due to our incomplete understanding of the geologic history of the Colorado Front Range, applying (U-Th)/He thermochronology to minerals with low closure temperatures has the potential to provide new information on the region's multistage history of exhumation and uplift. Previous apatite-fission track (AFT) work has shown that the Front Range cooled through temperatures of ~120 °C during Late Cretaceous to Early Tertiary time, corresponding to erosion of sedimentary cover from the basement during the Laramide Orogeny (Kelley and Chapin, 2004). However, no apatite (U-Th)/He (AHe) dating has been done in this area, despite its lower closure temperature (~70 °C), making it valuable for correlating time with depth since the apatite He system records some of the uppermost cooling in the crust (e.g., Wolf et al., 1998). AHe data used in conjunction with (U-Th)/He data from a mineral such as zircon that exhibits a higher closure temperature (nominally ~180 °C) can provide additional context for the timing and duration of exhumation (Reiners, 2005). Constraining the time at which minerals were at a sufficient depth to cool through their respective closure temperatures allows for the interpretation of a rock unit's exhumational history.

Although the basement rock of the Front Range formed in the Proterozoic, more recent thermal events like the Laramide Orogeny can reset their (U-Th)/He dates. For example, minerals within the Silver Plume Granite may have originally cooled in the Proterozoic, but sufficient thermal activity during the Early Tertiary may have heated the rock so that evidence of that earlier age is lost. By understanding the temperatures at which a mineral's age can be reset, it is possible to interpret when a rock unit cooled as it was exhumed to the surface, even if it took place long after the mineral formed. Mineral systems with low closure temperatures, such as apatite and zircon, are more easily reset than higher-temperature minerals, making them useful for examining recent cooling events. Obtaining (U-Th)/He dates for both apatite and zircon with different closure temperatures, and adding them to the available constraints from the AFT results, will

yield a more complete thermal history than if only one chronometer was applied. In this study I apply apatite and zircon (U-Th)/He thermochronology to better resolve the timing and magnitude of unroofing in the Colorado Front Range during the Laramide Orogeny.

Geologic Background

The geologic history of the Colorado Front Range is complex, with orogenic events beginning in the Proterozoic and ending in the Mid-Cenozoic (McMillan et al. 2006, Bickford et al. 1986). The modern Front Range is a Laramide uplift along the eastern margin of the Southern Rocky Mountains in Colorado, providing a dramatic backdrop for urban areas such as Denver where steep mountainous terrain transitions to the High Plains in the east (Figure 1). With a mean elevation of over 2 km, the Rocky Mountain orogenic belt extends across nearly 5,000 km of North America as a relic of the protracted tectonic history of the continent (McMillan et al., 2006).

The Colorado Front Range has undergone three major orogenic events. The first occurred in the Proterozoic (~1.75 Ga), where arc and back-arc assemblages generated plutonic and volcanic rocks, some of which were later metamorphosed (Bickford et al., 1986). These Proterozoic rocks remain as basement rock today, represented in the study area of the Front Range by the granodiorite of the Boulder Creek Batholith (~1.7 Ga), the schist and gneiss of the Idaho Springs Formation (~1.7 Ga), and the Silver Plume Granite (~1.4 Ga) (Gable, 1979).

The second major event occurred in the late Paleozoic and formed the Ancestral Rocky Mountains (Kluth et al., 1980). During this time, Precambrian basement rock was uplifted and exposed at the surface and was subsequently eroded as streams cut through the rising topography. The Front Range contains little evidence of this uplift in the form of emplaced igneous intrusions or plutons, but the Pennsylvanian and younger strata that lie unconformably over the Proterozoic basement rock represent the eroded material produced from the uplift. The first sedimentary formation to be deposited across this basement erosional surface was the sandstone of the Fountain Formation, which composes the iconic Flatirons formations of Boulder, Colorado. The climate became arid

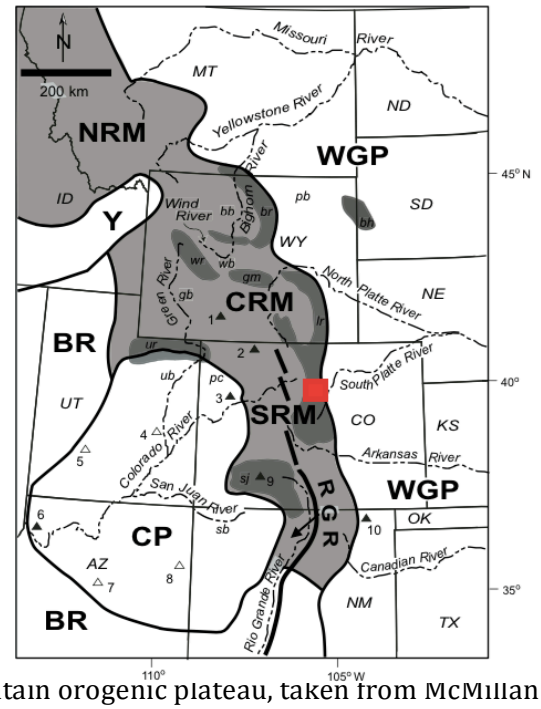

Figure 1. Rocky Mountain orogenic plateau, taken from McMillan et al. 2006. The Colorado Front Range is located in the Southern Rocky Mountains (SRM) where the South Platte River intersects the eastern margin of the orogenic plateau. The red box indicates the sampling area.

as Colorado sat on the western edge of the ancient continent Pangaea, generating fine-grained sandstones of the Lyons Formation that were deposited as eolian dunes (Cole et al., 2010). The climate in the Front Range would continue to change as more sedimentary layers were deposited throughout the Mesozoic. The development of the Western Interior Seaway during the Cretaceous created yet another shift in depositional environments, leading to the deposition of the Pierre Shale that now covers most of the undulating terrain just east of the mountains of the Front Range (Cole et al., 2010).

The most recent orogenic event began at the end of the Mesozoic (~70 Ma). Known as the Laramide Orogeny, this widespread uplift initiated yet another cycle of magmatic activity that heated and deformed the existing basement rock (Cole et al., 2010). This event led to tilting of the Late Paleozoic and Mesozoic strata to the east. Deformation of existing rock units and the intrusion of many dikes and sills in the area proceeded to convolute the geologic structure of the Front Range. Mantle-derived magmas were generated in the Front Range but were concentrated farther south than the study area, such as at Table Mountain in Golden, Colorado.

The Laramide Orogeny is thought to have ended by the mid-Paleogene (~40 Ma), creating a substantial amount of uplift and subsequent erosion of the uplifted rock throughout its duration (Kellogg et al., 2006). This represents a crucial time in the Front Range's history because it encompassed a period of large-scale uplift and exhumation that defines the modern Rockies and should be recorded in the thermochronological record. As crystalline basement rock was being uplifted, the exposed peaks of mountains at the surface were rapidly eroded. The removal of material from the top down allowed rocks to cool as they rose toward the surface, throughout which accessory minerals like apatite and zircon cooled through their respective closure temperatures. By evaluating multiple minerals with distinct closure temperatures in the same rock sample, it is possible to ascertain how much time passed between cooling of the higher temperature and the lower temperature minerals and infer the rate and timing of exhumation.

Background of Thermochronology

Thermochronology, a method of radiometric dating, has made a significant contribution to the understanding of thermal histories in a wide range of geologic settings. This set of techniques utilizes the decay rates of radioactive isotopes of elements like uranium and thorium in order to evaluate the amount of time that has passed since rocks have cooled below the temperature where the daughter product is retained. Unstable isotopes will radioactively decay into stable daughter isotopes at a known rate (represented by an isotope's 'half-life' in years), which is used to date a mineral by determining the ratio of daughter to parent elements since every atom of the daughter element in the sample must have formed through the decay of a parent atom. Once cooled, minerals can retain stable isotopes produced from decay chains as well as decay products like alpha particles that form through a decay process known as α-emission. Alpha particles are equivalent to ^{4}He and can be measured in the same way as a stable daughter isotope, but with the important exception that ^{4}He can diffuse out of a mineral at high enough temperatures. (U-Th)/He thermochronology takes advantage of the

radioactive isotopes of U and Th (and Sm to a lesser extent) that decay into ^{4}He at a known rate, providing a radiometric clock that starts once a mineral cools enough to prevent ^{4}He from escaping the crystal structure (Reiners, 2005). The temperature required for the complete retention of decay products within a crystal varies between minerals and is referred to as closure temperature.

In thermochronology, closure temperature refers to the temperature required to 'immobilize' the daughter products within a crystal (Dodson, 1973). As a crystal cools through its closure temperature, daughter products that were previously mobile become locked in the crystal lattice. Closure temperature is therefore a measure of the temperature sensitivity of a thermochronometer, and different thermochronometers have different temperature sensitivities. The closure temperature of the apatite He system is ~70 °C while the closure temperature for the zircon He system is ~180 °C. The closure temperature and calculated date of a thermochronometer can be used to interpret the geologic setting and time-temperature path undergone by a mineral. However, the production of radioactive decay products may affect the calculated date if a crystal has been damaged as a result of radioactive decay.

An understanding of the effects of radiation damage has been shown to be critical to the interpretation of (U-Th)/He dates from different minerals (e.g., Flowers et al., 2009; Guenthner et al., 2013). Zircon can accumulate damage as the parent isotopes radioactively decay, leading to a change in the ability for a crystal to retain the decay product ^{4}He (Guenther et al., 2013). The same is true for apatite, but to a lesser extent because of its lower concentrations of U and Th (Flowers et al., 2009). As zircon accumulates radiation damage from α-emission, its ability to retain helium is altered. Helium retentivity will increase until radiation doses become so large that the retentivity will begin to decrease, which is typically associated with visible degradation of the crystal (Reiners, 2005, Guenthner et al., 2013). The high degree to which zircons in the Proterozoic rocks sampled for this study have been damaged has led to an overall loss in their ability to retain helium.

Because U and Th produce ^{4}He in different quantities as they undergo α-emission, it is necessary to evaluate the total concentration of parent isotopes that can ultimately damage the crystal. To do this, the effective uranium concentration (eU) is

calculated in ppm as a weighted representation of the total concentration of unstable parent isotopes (eU = U + 0.235 × Th), making eU a suitable proxy for the amount of radiation damage a grain has accumulated (Flowers et al., 2009). A high eU may result in a loss of ^{4}He and a calculated age that is lower than expected since the number of decay products in the grain will not accurately reflect the total number of decay products that were produced. It can be useful to plot a grain's calculated (U-Th)/He date vs eU to evaluate the effect of radiation damage on a He dataset (Flowers et al., 2009). In zircon, for certain thermal histories, it is common to observe a trend of younger (U-Th)/He dates with increasing eU.

Chapter 2
Locations and Methods

Sample Locations and Their Geologic Context

MSc student Joshua Johnson and I performed fieldwork in the Colorado Front Range during the summer and winter of 2014. Sample locations extended from the interior of Rocky Mountain National Park (RMNP) to along its eastern margin within Big Thompson Canyon (Figure 2a). Two sets of samples were collected within the National Park that differed enough in geographic location and elevation to test whether they underwent distinct thermal histories due to variable exhumation. One set of samples was collected from an area along the Continental Divide near Mount Ida, and another set from the area of Lumpy Ridge just outside the city of Estes Park, Colorado. Lumpy Ridge is located ~25 km east and ~1 km lower than the Mount Ida region (Figure 2a).

A third set of samples was collected from within Big Thompson Canyon, located directly to the east of RMNP within the Front Range. The canyon was incised by the Big

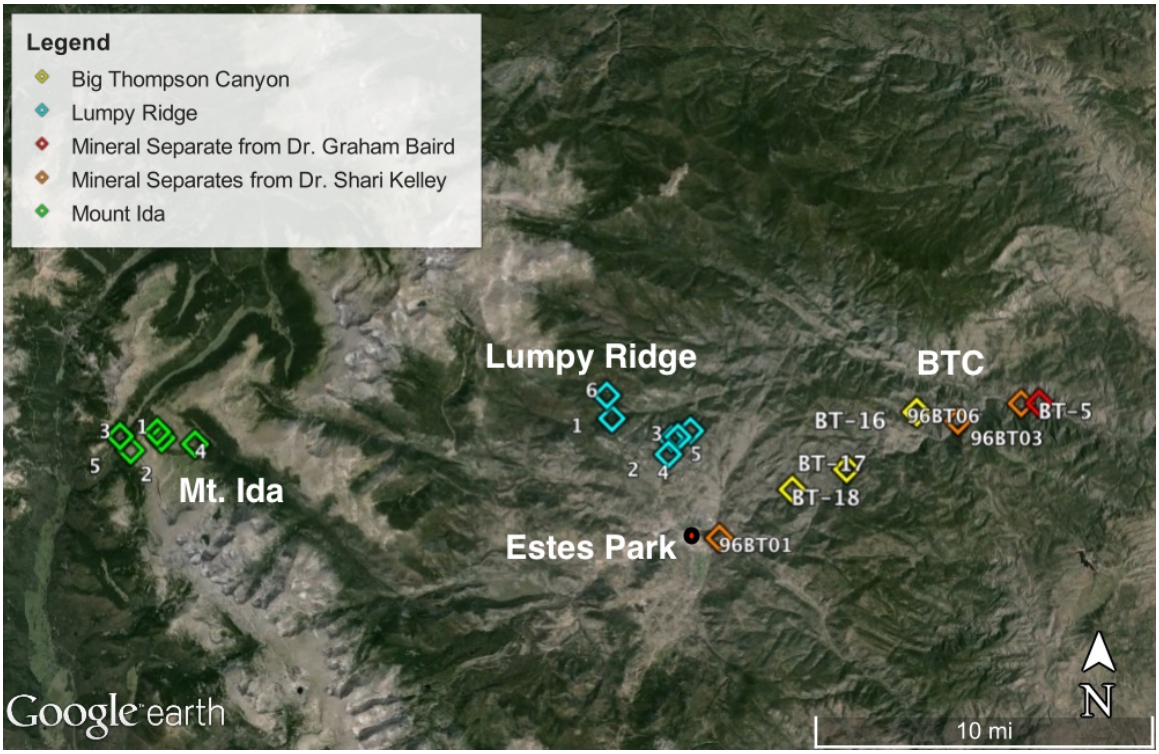

Figure 2a. Map of the sampling area in the Colorado Front Range. Five samples were collected in the vicinity of Mount Ida along the Continental Divide, six samples from Lumpy Ridge outside of Estes Park, and three samples from within Big Thompson Canyon. Dr. Shari Kelley and Dr. Graham Baird provided four additional mineral separates from Big Thompson Canyon.

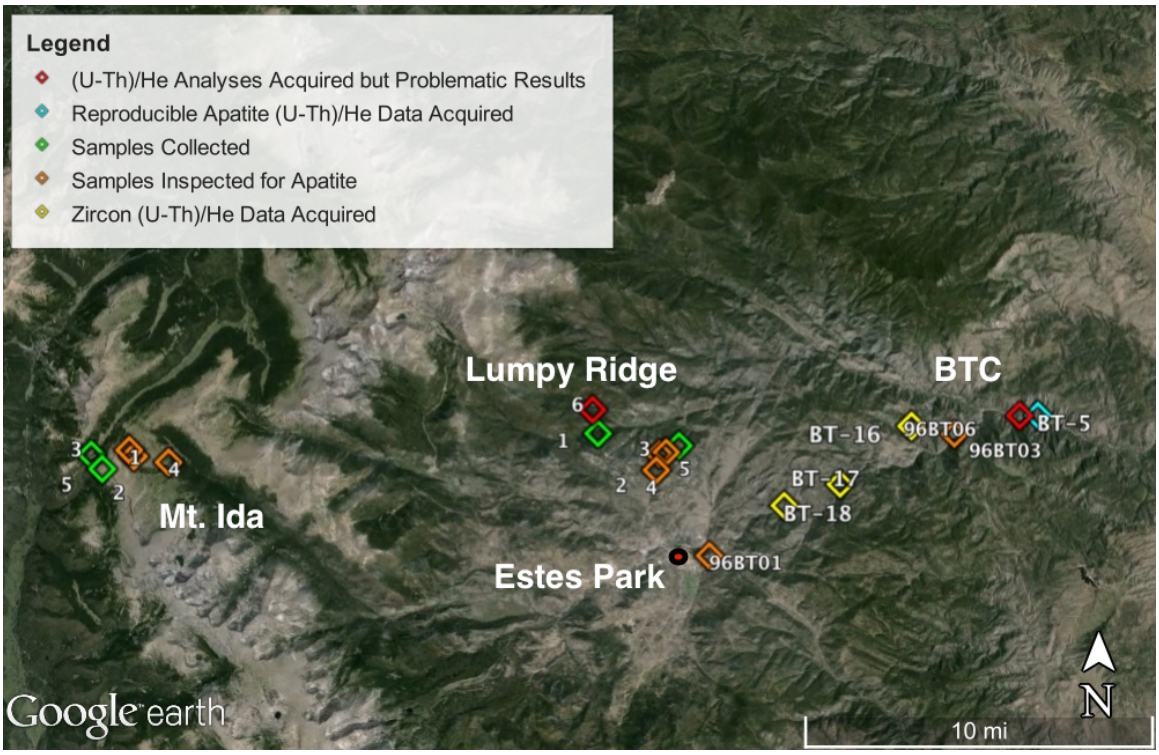

Figure 2b. Sampling locations are labeled as follows. Red– Apatite (U-Th)/He analyses were acquired but produced problematic results owing to inclusions. Blue– reproducible apatite (U-Th)/He data was acquired. Green– Samples were collected but not inspected because of low apatite content. Orange– Samples were collected and inspected for apatite. Yellow– Zircon (U-Th)/He data acquired.

Thompson River, a tributary of the South Platte. The river incision has exposed Proterozoic basement rock at an elevation comparable
to Lumpy Ridge in the upper canyon but considerably lower in elevation towards the mouth of the canyon. In order to provide date-elevation relationships, one sample was collected from an elevation ~275 m higher than the rest (Figures 3, 4).

Figure 3. Outcrop of the Boulder Creek Granodiorite in the sampling area of higher elevation within Big Thompson Canyon.

Figure 4. Sample BT-17 of the Boulder Creek Granodiorite. The Boulder Creek Granodiortie is medium-grained, equigranular, and has a dominant mineral assemblage of quartz, potassium feldspar, plagioclase feldspar, and biotite.

Samples and Methods

Rock types were targeted based on their potential for containing the uranium- and thorium-bearing accessory minerals apatite and zircon. These minerals occur in small quantities within most rocks, but are common in many felsic igneous rocks. However, these minerals are susceptible to chemical alteration during surface weathering. Radiometric techniques require a mineral's composition to remain constant so that the measured amount of decay product accurately reflects those generated only by the decay of the desired mineral and not from a replacement mineral. Therefore, surfaces of outcrops that had been visibly weathered (e.g., oxidation or surface staining) were avoided or kept to a minimum percentage of the total rock sample.

A hammer and chisel were used to collect ~5 kg samples from the three localities with elevations ranging from 2152 m to 3660 m (Figure 2a). The first six samples were collected in June of 2014 in the Lumpy Ridge area. The rock types sampled were

emplaced during the Proterozoic and included ~1.7 Ga biotite schist, pegmatite, and the ~1.4 Ga Silver Plume Granite. The range in elevation for these samples was 2613 m to 2700 m. We also sampled in the vicinity of Mount Ida along the Continental Divide. Six samples of similar size to those of Lumpy Ridge were collected, with a range in elevation from 3367 m to 3660 m. The same Proterozoic rock types as those sampled in Lumpy Ridge were located and collected. The final four samples were collected in Big Thompson Canyon approximately 5-10 km east of Estes Park (Figure 5). Although the first two localities required backpacking and strenuous hiking to locate minimally weathered outcrops, the deep incision of the Big Thompson River has left many areas of exposed bedrock that are more easily accessible. Two samples were collected from within the canyon (~2200 m elevation) and one from the top of a ridge outside of the canyon (2460 m elevation) to provide a vertical range in the samples. Several additional samples were provided as mineral separates by Dr. Shari Kelley and Dr. Graham Baird.

Standard mineral separation techniques were performed on 14 samples within the laboratories of the Department of Geological Sciences. This entailed multiple steps to reduce the volume of each rock sample with the intention of isolating the accessory minerals of apatite and zircon. The first step was to pulverize the samples between steel plates using a rock crusher to reduce as much of the sample as possible to grain sizes less than 500 μm. This smaller fraction was then subjected to density separation. The first of two steps that utilize the high density of these accessory minerals was performed using a Wilfley table, which works in the same way as simple panning techniques but in a mechanized fashion. This step can reduce the sample size by >90%, leaving only the minerals with highest densities.

The next procedure uses magnetic susceptibility to separate the remaining sample fraction, and is done on a Frantz using currents of up to 1.4 A. This step is useful for eliminating oxides and other minerals that have similar density but higher magnetic susceptibility than apatite or zircon. The second density separation procedure involves the use of the heavy liquid lithium metatungstate (LMT), which was kept at a density of ~2.85 g/cm^3. Once centrifuged in LMT, common minerals like quartz and feldspars that have densities below 2.85 g/cm^3 separate from the apatite and zircon, which have densities above 3 g/cm^3. Next, the remaining sample was subjected to yet another round

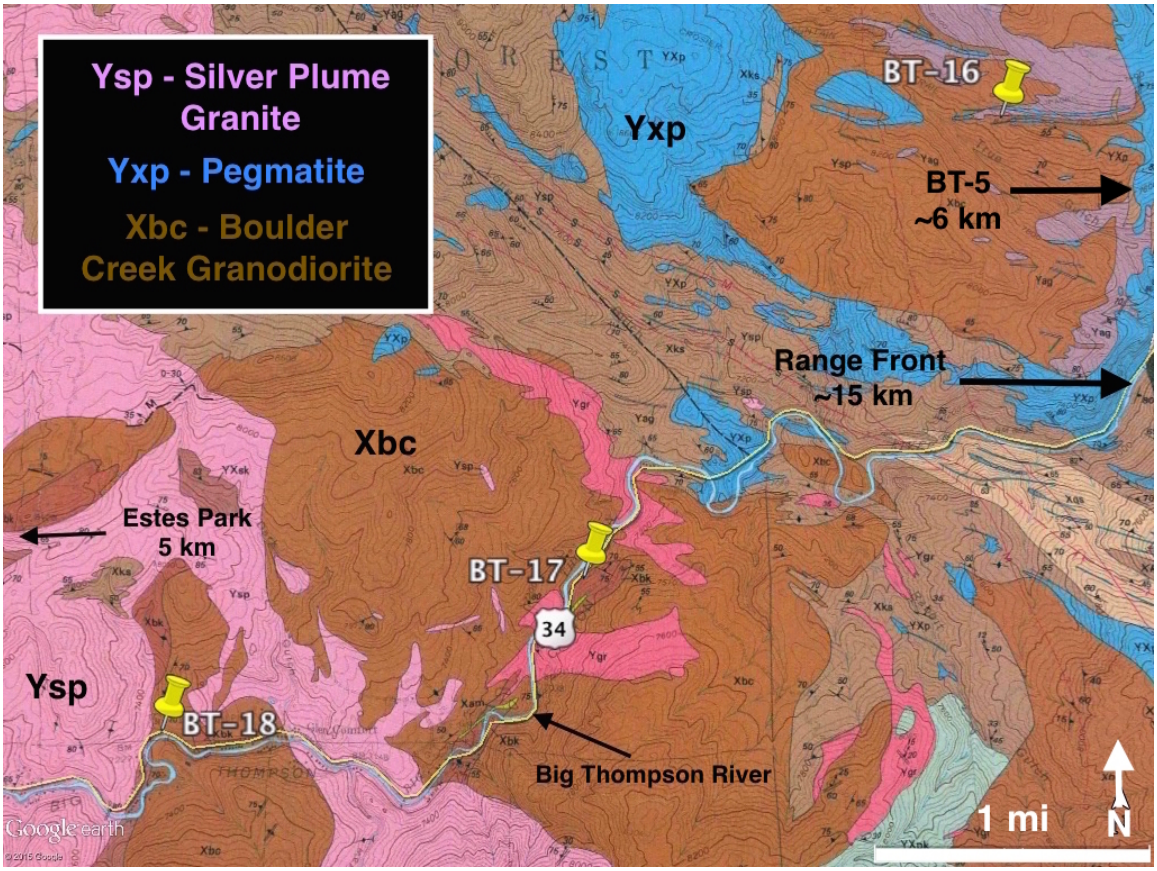

Figure 5. Samples BT-5, BT-16, BT-17, and BT-18 of the Boulder Creek Granodiorite were collected from Big Thompson Canyon and are the samples for which I acquired data. Sample locations are superimposed on the "Geologic map of the Glen Haven quadrangle, Larimer County, Colorado, 1989 (Cole and Braddock)". Boulder Creek Granodiorite is ~1.7 Ga, Silver Plume Granite ~1.4 Ga, and pegmatite ~1.4 Ga.

of magnetic separation, but using stronger currents through the magnet and a higher inclination of the platform used for grains to pass by the magnet. This final step yields minute fractions of the sample that can then be scrutinized and picked through using an optical microscope to select suitable grains for analysis.

Grains were chosen for analysis based on their size, shape, and inclusion-free character. A crucial correction that needs to be made is for the ejection of alpha particles (or ^{4}He atoms) that are propelled ~20 um from the site of radioactive decay of uranium and thorium (Farley, 2000). There is an increasing probability that alpha particles will be ejected from the mineral the closer they are to the edge of the grain. Thus, analyzed grains must be of a minimum size, and the crystals are measured to determine this alpha-

ejection correction. Euhedral crystals were favored because anhedral crystals produce complications when applying this correction. Lastly, grains with mineral inclusions were avoided when possible to prevent erroneous measurements of the parent and daughter nuclides. Problematic results owing to inclusions are more common in apatite analyses than zircon because of the different strengths of acids that are used to dissolve each mineral. The series of acids required to dissolve zircon will also dissolve the inclusions, but the weaker acid used for apatite will not dissolve the inclusions since they are typically composed of the resistant mineral zircon (Vermeesch et al., 2006).

I inspected 11 samples for inclusion-free apatites (Figure 2b). Three samples were from Mount Ida, four from Lumpy Ridge, three were provided by Dr. Shari Kelley, and one was from Dr. Graham Baird. Of the 11 inspected samples, (U-Th)/He analyses were acquired for two of them. One sample was from Lumpy Ridge and the other was from Big Thompson Canyon. Both samples produced problematic results due to inclusions. Given the abundance of inclusions in the apatite samples, standards for requiring apatites to be inclusion-free were relaxed. Apatite (U-Th)/He analyses were acquired for sample BT-5 with apatites selected for having as few a number of inclusions as I could find. In addition to the initial 11 samples inspected for inclusion-free apatites, samples BT-16, BT-17, and BT-18 were inspected for apatite. Since these three samples did not have inclusion-free apatites, zircon (U-Th)/He analyses were acquired instead.

The initial goal of this study was to analyze apatites from the same samples that Joshua Johnson used for his study, which focused on zircon rather than apatite. However, because of the paucity of high-quality apatites in those samples, I collected three additional samples (BT-16, BT-17, BT-18) from a new rock unit, the Boulder Creek Granodiorite, with the intention of obtaining inclusion-free apatite grains. The mineral separates from these samples revealed apatites with a prevalence of inclusions equal to, if not exceeding, those from the other lithologies. I therefore analyzed zircons from these samples instead.

Five individual grains were analyzed from each sample in order to check data reproducibility. The selected apatite grains were packed into hollow platinum tubes that provided a protective packet around each grain. Zircons underwent the same procedure but were packed into tubes made of niobium. These packets were then subjected to

heating by a diode laser within a quadrupole mass spectrometer, which degassed the grain of all its ^{4}He. The non-radiogenic isotope ^{3}He was added as a spike in a known quantity to provide a baseline measurement for the mass spectrometer. Likewise, apatites and zircons with known ages were also run as standards to ensure the machine was producing accurate measurements. The degassed grains were then subjected to a final stage of analysis in an inductively coupled plasma mass spectrometer (ICP-MS) that measured the amounts of the parent isotopes uranium, thorium, and samarium. Each grain was dissolved in acid before entering the ICP-MS, with apatite being dissolved in only HNO_3 and zircon in a sequence of HF, HCl, and HNO_3. The ratios of the parent to daughter nuclides and the appropriate half-lives were then entered into radioactive decay equations within a spreadsheet. Lastly, the alpha ejection correction was applied based on the grain measurements.

Chapter 3
Results

Results

The (U-Th)/He dates calculated from all samples are Late Cretaceous to Early Tertiary. The data is summarized in Table 1.

Sample BT-5 from Big Thompson Canyon yielded 9 reproducible apatite analyses with a mean date and uncertainty of 66.5 ± 9.62 Ma. Two analyses are not reported in Table 2, because one apatite was too small, and the other was not apatite. The remaining analyses yield broadly uniform dates uncorrelated with apatite eU (Figure 6).

In contrast, the inclusion-bearing apatite grains from sample LR-6 from Lumpy Ridge produced irreproducible data. We therefore exclude these samples from the discussion below. A significant limitation of dating apatites using (U/Th)/He thermochronometry stems from the occurrence of 'parentless' helium within the crystal structure. As unstable cations that have substituted into the crystal structure of apatite radioactively decay, the decay product is found in quantities proportional to the amount of the parent isotope (i.e.

Sample	Mineral	Elevation (m)	Age Range (Ma)	Average Age (Ma)	Uncertainty (Ma)
BT-5	Apatite	1784	49.10 ± 3.53 - 80.92 ± 6.62	66.52	9.62
BT-16	Zircon	2460	41.18 ± 2.95 - 74.52 ± 8.42	57.19	14.04
BT-17	Zircon	2152	32.50 ± 2.30 - 51.10 ± 5.09	45.02	7.24
BT-18	Zircon	2222	55.59 ± 3.95 - 83.94 ± 6.34	64.55	11.13

Table 1. Summary of age and elevation for the four samples that produced usable data.

every atom of ^{4}He represents a U, Th, or Sm atom that has decayed). However, it is possible (and quite common) for another U/Th-bearing mineral such as zircon to grow within an apatite as a
mineral inclusion (Figures 7, 8) (Vermeesch et al., 2006). As the U and Th within the inclusion radioactively decay, He is produced and can be ejected from the inclusion into the crystal structure of the surrounding apatite. To prepare an apatite grain for analysis in the ICP-MS it is dissolved in HNO_3 to release the non-gaseous U and Th. The issue with this procedure is that more resistant minerals like zircon do not dissolve in HNO_3 (they require a series of stronger acids) and the parent isotopes like U and Th will not be liberated and analyzed from the inclusion. This can lead to the measurement of ^{4}He that was produced by the inclusion since some of it was ejected into the apatite structure, but the parent isotopes of U and Th *not* being measured since they are trapped within the un-dissolved inclusion. The end result is that the measurement of 'parentless' helium can increase the (U-Th)/He dates because the quantity of decay product is disproportionately large.

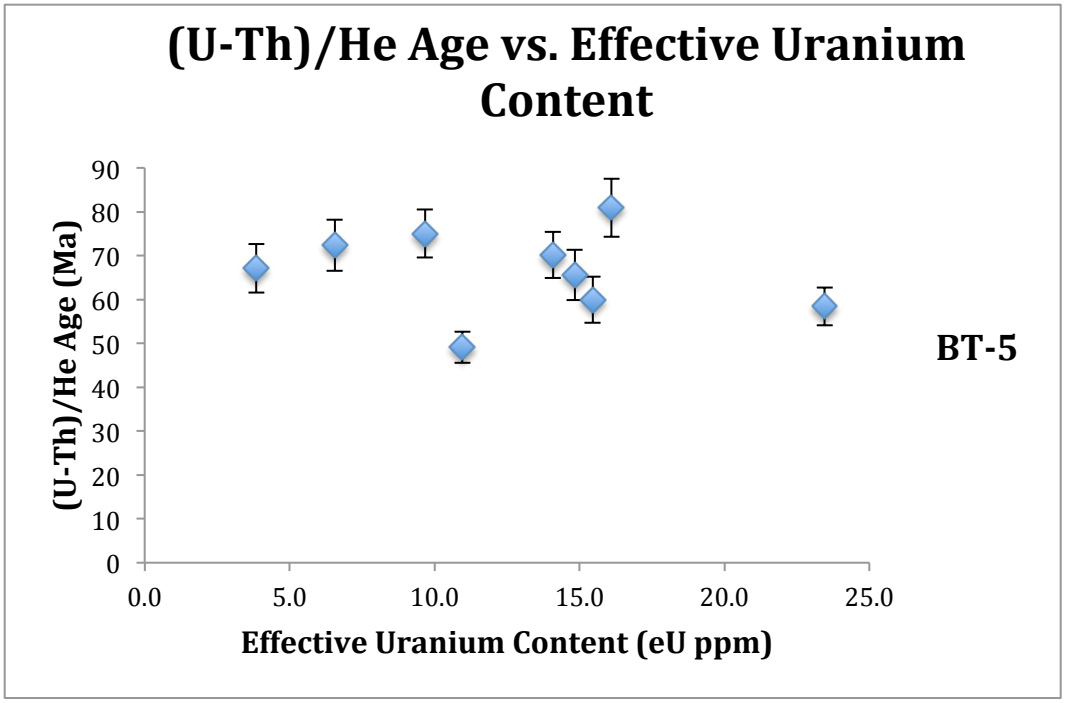

Figure 6. Corrected age vs. effective uranium content (eU) for apatite in sample BT-5. There is little to no correlation between age and eU within this sample.

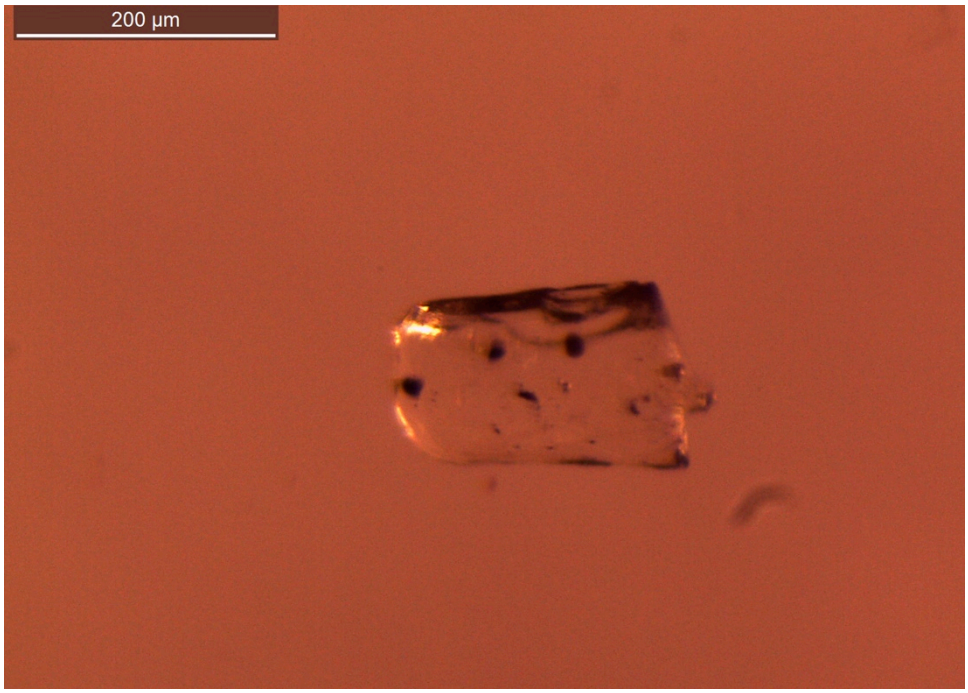

Figure 7. Apatite from sample LR-2 of the Silver Plume Granite collected from Lumpy Ridge. Inclusions are visible as dark spots within the grain. The image was taken using reflected light.

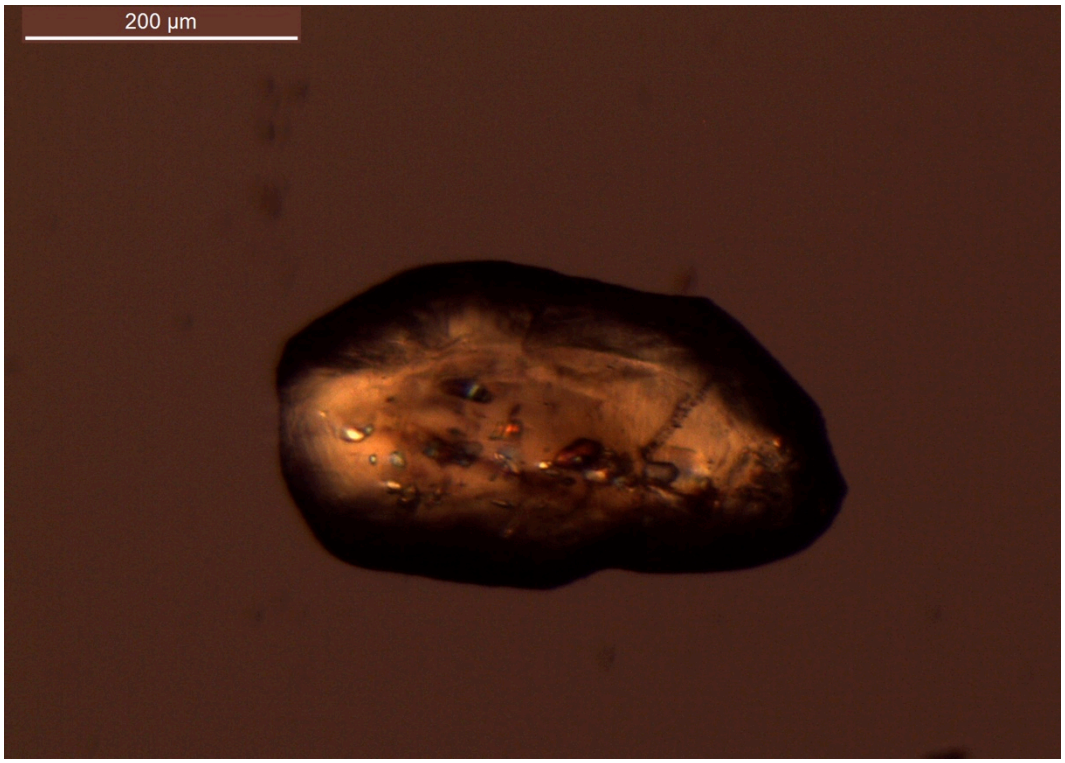

Figure 8. Apatite from sample BT-17 of the Boulder Creek Granodiorite collected from Big Thompson Canyon showing numerous mineral inclusions, viewed in cross-polarized light through an optical microscope.

Zircon (U-Th)/He analyses were acquired for three samples. Sample BT-16 has a mean (U-Th)/He date of 57.19 ± 14.04 Ma, sample BT-17 has a mean date of 45.02 ± 7.24 Ma, and sample BT-18 has a mean date of 64.55 ± 11.13 Ma (Table 3). There is a negative correlation between the individual ZHe dates and eU values for the three samples (Figure 9). This is expected in zircon because radiation damage can lower He retentivity. The zircon (U-Th)/He dates are Early Tertiary.

Sample Name	length 1 (μm)	width 1 (μm)	length 2 (μm)	width 2 (μm)	2X Term	Dim Mass (μg)	rs (μm)	4He (nmol/g)	±	U (ppm)	±	Th (ppm)	±	Sm (ppm)	±	eU
BT-5_ap03	194.7	107.1	195.6	93.6	Y	4.08	59.84	1.073	0.004	3.41	0.18	1.88	0.02	25.67	0.97	**3.8**
BT-5_ap04	166.1	90	167.5	80.9	Y	2.53	50.98	4.961	0.013	13.12	0.37	12.70	0.30	61.12	1.68	**16.1**
BT-5_ap05	245.1	132.6	240.4	119	Y	7.98	75.08	2.314	0.004	7.96	0.18	12.76	0.22	34.13	0.71	**11.0**
BT-5_ap06	131.6	100.1	132.7	88.4	Y	2.44	52.05	5.228	0.015	19.33	0.54	17.56	0.49	61.79	3.18	**23.5**
BT-5_ap07	196	87.2	178.4	79.9	Y	2.72	51.65	3.526	0.012	11.49	0.43	16.87	0.93	59.22	2.03	**15.4**
BT-5_ap08	165.2	87	166.3	81.8	Y	2.45	50.42	3.673	0.009	12.96	0.52	7.98	0.22	43.56	2.33	**14.8**
BT-5_ap09	234.8	107.9	233.3	91.4	Y	4.83	61.65	4.028	0.006	11.78	0.37	9.83	0.45	48.63	0.86	**14.1**
BT-5_ap10	145.8	102.6	142.3	89.3	Y	2.76	54.15	1.870	0.014	5.87	0.27	2.90	0.17	28.67	2.92	**6.6**
BT-5_ap11	309.6	138.6	308.7	120.4	Y	10.78	80.33	3.179	0.004	8.35	0.20	5.63	0.20	26.58	0.48	**9.7**

Table 2. Apatite (U-Th)/He data for sample BT-5 from Big Thompson Canyon.

Sample Name	4He (ncc)	±	U (ng)	±	Th (ng)	±	Sm (ng)	±	Th/U	Raw Date (Ma)	±	Ft	± (%)	Corrected Date (Ma)	Full Unc. (Ma)	Analyt. Unc. (Ma)
BT-5_ap03	0.098	0.000	0.014	0.001	0.008	0.000	0.105	0.004	0.551	48.80	2.13	0.727	7.0	67.11	5.53	2.13
BT-5_ap04	0.282	0.001	0.033	0.001	0.032	0.001	0.155	0.004	0.968	55.14	1.23	0.681	7.9	80.92	6.62	1.23
BT-5_ap05	0.414	0.001	0.064	0.001	0.102	0.002	0.272	0.006	1.603	38.01	0.63	0.774	7.0	49.10	3.53	0.63
BT-5_ap06	0.286	0.001	0.047	0.001	0.043	0.001	0.151	0.008	0.908	40.31	0.91	0.690	7.0	58.42	4.30	0.91
BT-5_ap07	0.215	0.001	0.031	0.001	0.046	0.003	0.161	0.006	1.469	40.85	1.22	0.681	8.3	59.98	5.29	1.22
BT-5_ap08	0.202	0.000	0.032	0.001	0.020	0.001	0.107	0.006	0.616	44.67	1.50	0.681	8.1	65.63	5.76	1.50
BT-5_ap09	0.436	0.001	0.057	0.002	0.047	0.002	0.235	0.004	0.834	51.33	1.34	0.732	7.0	70.15	5.24	1.34
BT-5_ap10	0.116	0.001	0.016	0.001	0.008	0.000	0.079	0.008	0.493	50.88	2.04	0.703	7.0	72.38	5.84	2.04
BT-5_ap11	0.768	0.001	0.090	0.002	0.061	0.002	0.286	0.005	0.675	59.33	1.19	0.791	7.0	75.01	5.46	1.19

Table 2 (continued).

Sample Name	length 1 (μm)	width 1 (μm)	length 2 (μm)	width 2 (μm)	2X Term	Dim Mass (μg)	rs (μm)	4He (nmol/g)	±	U (ppm)	±	Th (ppm)	±	eU
BT-16_zir01	526	88.4	527.4	99	Y	21.43	64.53	189.223	0.098	991.40	16.49	195.37	3.27	**1037.32**
BT-16_zir02	283.1	68.1	283.3	81.3	Y	7.29	49.50	144.638	0.171	459.31	4.63	26.54	0.27	**465.55**
BT-16_zir03	186.4	84	184.2	71.4	Y	5.17	48.22	134.868	0.202	606.78	10.71	68.90	1.22	**622.97**
BT-16_zir04	183.2	82.8	183.4	81.5	Y	5.75	50.33	123.164	0.092	462.36	7.46	99.48	1.62	**485.74**
BT-16_zir05	179.9	59.9	176.9	62.4	Y	3.10	39.20	134.102	0.148	309.12	6.60	51.83	1.11	**321.30**
BT-17_zir01	279.8	79	274	77.5	Y	7.88	51.49	156.537	0.148	710.41	9.95	76.57	1.08	**728.40**
BT-17_zir02	285.8	85.6	285.5	88	Y	10.01	56.52	132.233	0.104	650.55	8.52	41.45	0.55	**660.29**
BT-17_zir03	341.9	88.6	342.1	67.9	Y	9.57	52.66	303.453	0.202	1499.87	49.75	174.96	5.84	**1540.99**
BT-17_zir04	401.6	84.2	403.9	75.9	Y	11.97	54.60	209.441	0.189	990.24	15.18	97.15	1.50	**1013.07**
BT-17_zir05	587.7	94.1	585.9	88.5	Y	22.72	63.54	264.333	0.231	1799.88	18.94	181.68	1.93	**1842.58**
BT-18_zir01	344.7	93.5	345.3	82.5	Y	12.37	58.53	243.531	0.109	613.98	9.50	227.78	3.55	**667.50**
BT-18_zir02	287.8	114.4	287.2	89.9	Y	13.75	65.07	88.610	0.055	296.31	5.81	108.20	2.14	**321.74**
BT-18_zir03	503.4	151	504.4	149.4	Y	52.86	98.03	102.190	0.053	318.52	5.36	129.01	2.18	**348.84**
BT-18_zir04	488.2	130.7	489.4	125	Y	37.13	84.79	184.991	0.136	586.89	6.02	338.58	3.50	**666.46**
BT-18_zir05	328.7	88.7	328.2	102.1	Y	13.83	62.48	115.974	0.102	449.87	5.97	101.37	1.35	**473.70**

Table 3. Zircon (U-Th)/He data for samples BT-16, BT-17, and BT-18 from Big Thompson Canyon.

Sample Name	4He (ncc)	±	U (ng)	±	Th (ng)	±	Th/U	Raw Date (Ma)	±	Ft	± (%)	Corrected Date (Ma)	Full Unc. (Ma)	Analytic Unc. (Ma)
BT-16_zir01	90.91	0.0	21.250	0.353	4.188	0.129	0.197	33.76	0.52	0.820	7.0	41.18	2.95	0.52
BT-16_zir02	23.64	0.0	3.349	0.034	0.194	0.004	0.058	57.38	0.56	0.770	11.3	74.52	8.42	0.56
BT-16_zir03	15.62	0.0	3.136	0.055	0.356	0.004	0.114	40.05	0.67	0.764	10.1	52.40	5.35	0.67
BT-16_zir04	15.88	0.0	2.659	0.043	0.572	0.009	0.215	46.87	0.70	0.773	8.7	60.65	5.33	0.70
BT-16_zir05	9.32	0.0	0.958	0.020	0.161	0.005	0.168	76.94	1.54	0.715	18.9	107.61	20.42	1.54
BT-17_zir01	27.66	0.0	5.600	0.078	0.604	0.009	0.108	39.75	0.53	0.778	9.9	51.10	5.09	0.53
BT-17_zir02	29.65	0.0	6.509	0.085	0.415	0.007	0.064	37.06	0.46	0.797	7.6	46.52	3.59	0.46
BT-17_zir03	65.07	0.0	14.349	0.476	1.674	0.030	0.117	36.44	1.14	0.783	9.9	46.56	4.82	1.14
BT-17_zir04	56.18	0.1	11.852	0.182	1.163	0.020	0.098	38.25	0.56	0.790	9.3	48.43	4.55	0.56
BT-17_zir05	134.63	0.1	40.900	0.430	4.128	0.094	0.101	26.57	0.27	0.818	7.0	32.50	2.30	0.27
BT-18_zir01	67.55	0.0	7.598	0.118	2.819	0.068	0.371	67.30	0.94	0.802	7.4	83.94	6.34	0.94
BT-18_zir02	27.31	0.0	4.074	0.080	1.488	0.025	0.365	50.87	0.89	0.820	7.0	62.00	4.47	0.89
BT-18_zir03	121.07	0.1	16.837	0.283	6.819	0.183	0.405	54.09	0.81	0.878	7.0	61.58	4.41	0.81
BT-18_zir04	153.97	0.11	21.794	0.224	12.573	0.199	0.577	51.26	0.46	0.86	7.00	59.62	4.21	0.46
BT-18_zir05	35.95	0.03	6.222	0.083	1.402	0.025	0.225	45.26	0.56	0.81	7.00	55.59	3.95	0.56

Table 3 (continued)

Chapter 4
Discussion

Discussion

The mean apatite and zircon (U-Th)/He dates overlap within uncertainty and are Late Cretaceous to Early Tertiary in age. Significant uplift and heating of the Proterozoic basement of the Front Range started ~70 Ma with the onset of the Laramide Orogeny, and is thought to have ended by ~45 Ma (Kellogg et al., 2004). Thus the mean apatite and zircon dates, which range from 45.02 ± 7.24 Ma to 66.52 ± 9.62 Ma, overlap with or slightly postdate the Laramide Orogeny.

Because apatite (U-Th)/He data have a temperature sensitivity of ~70 °C, the AHe dates record Laramide cooling through temperatures of ~70 °C. This temperature is lower than the ~120 °C temperature previously constrained through AFT work (Kelley and Chapin, 2004). Therefore, the dates produced in this study are representative of the last stages of cooling as erosion intensified at the end of the Cretaceous. Assuming a typical geothermal gradient of ~25 °C/km, this result would imply that the Front Range basement was exhumed to depths of < 3 km by the end of the Mesozoic during the Laramide.

The similar He dates for the apatites and zircons, despite the substantial difference between their typical closure temperatures of ~70 °C and 180 °C, suggests rapid cooling through the zircon and apatite closure temperatures. It was initially anticipated that the studied apatites and zircons would have different (U-Th)/He dates because they are characterized by significantly different He closure temperatures when undamaged. The ZHe data could be reflective of the zircons passing through their nominal ~180 ˚C closure temperature at different times, indicating differential rates of cooling within a relatively small area of the Front Range. However, it is possible that significant radiation damage accumulation has substantially reduced the He retentivity of zircon, causing the zircons to

record a temperature that is lower than the temperature at which undamaged zircon would retain its helium (~180 °C) (Guenthner et al., 2013).

Joshua Johnson acquired ZHe data from sample BT-5 and found dates that were younger than the AHe dates I acquired from the same sample, which suggests the closure temperature of zircon was lower than apatite. These data are reinforced by recent experimental work done by Guenthner that indicate radiation damage could cause a significant decrease in He retentivity in zircon and could cause ZHe dates to be younger than those found using the AHe system. This is further substantiated by existing AFT work in the Front Range indicating that although the Front Range was reheated prior to the Laramide due to burial, the temperatures did not exceed ~130 ˚C and therefore did not

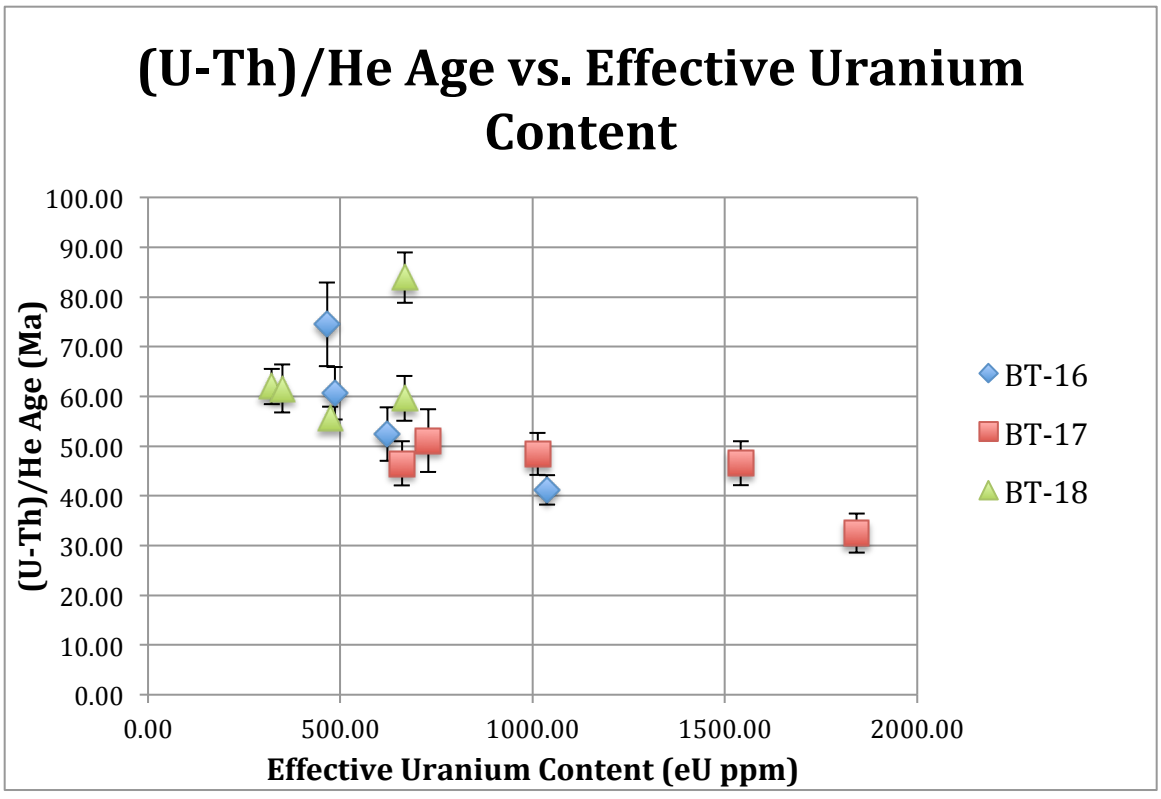

Figure 9. Corrected age vs. effective uranium concentration (eU) for samples BT-16, 17, and 18. It's evident that there is a correlation between age and eU, where age decreases with effective uranium content. Grain BT-16_zir01 has a high eU and may have undergone enough radiation damage so that the date calculated is younger than the date that the grain actually passed through its closure temperature.

reach the required ~180 ˚C closure temperature required to reset the dates of undamaged zircon. However, without performing further analysis to quantify the accumulation of radiation damage beyond the negative correlation of (U-Th)/He date vs. eU observed in Figure 9, the data can most easily be explained by a rapid cooling from ~180 ºC to 70 ºC as a result of Late Cretaceous–Early Tertiary uplift of the Front Range.

Future work in the Colorado Front Range can benefit from using low-temperature (U-Th)/He thermochronometry because of its ability to constrain timing and rates of exhumation at shallow depths. Work performed using multiple sampling areas and elevations could provide date-elevation relationships and estimates for exhumation rates. However, after studying samples collected from multiple rock units within the Front Range, the use of the apatite He thermochronometer may be limited due to the abundance of mineral inclusions within apatites in common Front Range lithologies. Their high occurrence limits the number of grains within a mineral separate that can be dated with reproducible results, and many hours of additional work are required to search through mineral separates for apatites with fewer inclusions. Applying He thermochronometers that record temperatures higher than the zircon and apatite He systems could provide additional constraints on the timing of exhumation since this would account for temperatures recorded at lower depths. Then the cooling history of the Front Range could be constrained throughout intervals of the Laramide Orogeny other than the one reflected by this study, or during the same time but at greater depth. The combination of the Colorado Front Range's complicated geologic history and popularity as a tourist attraction will only make the region more enticing for future research. Exploration into the causes, timing, and rate of Laramide exhumation will benefit both researchers and visitors alike as the rich history of the Rocky Mountains is further discovered.

References

Bickford, M. E., Van Schmus, ,W.R., & Zietz, I. (1986). Proterozoic history of the midcontinent region of North America. *Geology (Boulder), 14*(6), 492-496.

Chapin, C. E., & Kelley, S. A. (1997). In Bolyard D. W., Sonnenberg S. A. (Eds.), The Rocky Mountain Erosion Surface in the Front Range of Colorado*, Rocky Mountain Association of Geologists*, Denver, CO.

Cole, J.C., and Braddock, W.A. (2009). Geologic map of the Estes Park 30' x 60' quadrangle, north-central Colorado, *U.S. Geological Survey Scientific Investigations Map 3039,* 1 sheet, scale 1:100,000, pamphlet, 56 p.

Cole, J. C., Trexler,James H.,,Jr, Cashman, P. H., Miller, I. M., Shroba, R. R., Cosca, M. A., & Workman, J. B. (2010). Beyond Colorado's Front Range: A new look at Laramide basin subsidence, sedimentation, and deformation in north-central Colorado. *GSA Field Guide, 18*, 55-76.

Cross, T. A. and Pilger Jr., R. H. (1978). Constraints on absolute motion and plate interaction inferred from Cenozoic igneous activity in the western United States, *American Journal of Science,* 278(7): 865-902.

Dodson, M. H. (1973). Closure temperature in cooling geochronological and petrological systems. *Contributions to Mineralogy and Petrology, 40*(3), 259-274.

Farley, K. A. (2003). Problematic samples for apatite (U-th)/He dating; some possible causes and solutions. *EOS, Transactions, American Geophysical Union, 84*(46), Abstract V22G-06.

Flowers, R. M., Ketcham, R. A., Shuster, D. L., & Farley, K. A. (2009). Apatite (U-th)/He thermochronometry using a radiation damage accumulation and annealing model. *Geochimica Et Cosmochimica Acta, 73*(8), 2347-2365.

Gable, D. J. (1980). The Boulder Creek Batholith, Front Range, Colorado. *U.S.Geological Survey Professional Paper,*88.

Guenthner, W. R., Reiners, P. W., Ketcham, R. A., Nasdala, L., & Giester, G. (2013). Helium diffusion in natural zircon; radiation damage, anisotropy, and the interpretation of zircon (U-Th)/He thermochronology. *American Journal of Science, 313*(3), 145-198.

Kelley, S. A. (2002). Unroofing of the southern front range, Colorado; a view from the Denver Basin. *Rocky Mountain Geology,37*(2), 189-200.

Kelley, S. A., Chapin, C. E., Cather, S. M., & McIntosh, W. C. (2004). Denudation history and internal structure of the Front Range and Wet Mountains, Colorado, based on apatite-fission-track thermochronology. *Bulletin - New Mexico Bureau of Geology & Mineral Resources,* , 41-78.

Kellogg, K. S., Bryant, B., & Reed,John C.,,Jr. (2004). The Colorado Front Range; anatomy of a Laramide uplift. *GSA Field Guide,5*, 89-108.

McMillan, M. E., Heller, P. L., & Wing, S. L. (2006). History and causes of post-Laramide relief in the Rocky Mountain orogenic plateau. *Bulletin of the Geological Society of America, 118*(3), 393-405.

Reiners, P. W. (2005). Zircon (U-Th)/He thermochronometry. *Reviews in Mineralogy and Geochemistry, 58*(1), 151-179.

Vermeesch, P., Seward, D., Latkoczy, C., Wipf, M., Guenther, D., & Baur, H. (2007). Alpha - emitting mineral inclusions in apatite, their effect on (U-th)/He ages, and how to reduce it. *Geochimica Et Cosmochimica Acta, 71*(7), 1737-1746.

Wolf, R. A., Farley, K. A., & Kass, D. M. (1998). Modeling of the temperature sensitivity of the apatite (U-th)/He thermochronometer. *Chemical Geology, 148*(1-2), 105-114.